RESEARCH

GALNT9 enrichment attenuates MPP⁺-induced cytotoxicity by ameliorating protein aggregations containing α-synuclein and mitochondrial dysfunction

Yuanwen Peng[2†], Jun Liu[2,4†], Lili Sun[1], Qiuying Zheng[2], Can Cao[2], Wenyong Ding[1], Shufeng Yang[3], Li Ma[2*] and Wenli Zhang[1*]

Abstract

Background GALNTs (UDP-GalNAc; polypeptide N-acetylgalactosaminyltransferases) initiate mucin-type O-GalNAc glycosylation by adding N-GalNAc to protein serine/threonine residues. Abnormalities in O-GalNAc glycosylation are involved in various disorders such as Parkinson's disease (PD), a neurodegenerative disorder. GALNT9 is potentially downregulated in PD patients.

Methods To determine whether GALNT9 enrichment ameliorates cytotoxicity related to PD-like variations, a pcDNA3.1-*GALNT9* plasmid was constructed and transfected into SH-SY5Y cells to establish a GALNT9-overexpressing cell model.

Results Downregulation of GALNT9 and O-GalNAc glycosylation was confirmed in our animal and cellular models of PD-like variations. GALNT9 supplementation greatly attenuated cytotoxicity induced by MPP⁺ (1-Methyl-4-phenylpyridinium iodide) since it led to increased levels of tyrosine hydroxylase and dopamine, reduced rates of apoptosis, and significantly ameliorated MPP⁺-induced mitochondrial dysfunction by alleviating abnormal levels of mitochondrial membrane potential and reactive oxygen species. A long-lasting mPTP (mitochondrial permeability transition pores) opening and calcium efflux resulted in significantly lower activity in the cytochrome C-associated apoptotic pathway and mitophagy process, signifying that GALNT9 supplementation maintained neuronal cell health under MPP⁺ exposure. Additionally, it was found that glycans linked to proteins influenced the formation of protein aggregates containing α-synuclein, and GALNT9 supplement dramatically reduced such insoluble protein aggregations under MPP⁺ treatment. Glial GALNT9 predominantly appears under pathological conditions like PD-like variations.

---

†Yuanwen Peng and Jun Liu contributed equally to this work.

*Correspondence:
Li Ma
mali_lele@sina.com
Wenli Zhang
zhangwenli@dmu.edu.cn
Full list of author information is available at the end of the article

Conclusions GALNT9 enrichment improved cell survival, and glial GALNT9 potentially represents a pathogenic index for PD patients. This study provides insights into the development of therapeutic strategies for the treatment of PD.

Keywords GALNT, Glycosylation, Parkinson's disease, Mitochondrial dysfunction, A-synuclein

Introduction

Protein post-translational modifications (PTMs), the covalent addition of functional groups or the proteolytic cleavage of regulatory subunits of entire proteins, increase the functional diversity of the proteome and influence cell biology and pathogenesis. PTMs include various alterations, such as phosphorylation, glycosylation, ubiquitination, nitrosylation, methylation, acetylation, lipidation, and proteolysis. Among these, glycosylation is the most important form of PTMs.

Protein glycosylation is acknowledged as the most complex PTM because the addition of glycans is involved in a large number of enzymatic processes. It is becoming increasingly evident that glycosylation plays important roles in the functional diversification of proteins, and exerts significant effects on the conformation, folding, activity, distribution, and stability of proteins [1]. Based on the nature of the glycan–peptide bond and attached oligosaccharide, the most prominent forms of glycosylation events are N-, O-, and C-linked glycosylation and glycosylation. Among these four forms, O-glycosylation is one of the most commonly detected and plays a fundamental role in cell biology. In particular, O-glycosylation is essential for the biosynthesis of mucin-type proteins, a protein family with extensive O-glycosylation and high molecular weights.

O-glycosylation occurs post-translationally involving serine/threonine side chains of proteins in the Golgi apparatus. O-GalNAc is an important O-glycosylated residue. Mucin-type proteins trafficked into the Golgi apparatus are often O-glycosylated by N-acetylgalactosamine (GalNAc) transferase, which transfers a single GalNAc residue to the hydroxyl group of the serine/threonine residues of a protein.

Currently, GALNTs (UDP-GalNAc: polypeptide N-acetylgalactosaminyltransferases) are globally accepted as a family of GalNAc transferases responsible for mucin-type O-GalNAc glycosylation of proteins. GALNTs initiate mucin-type O-GalNAc glycosylation via catalyzing GalNAc transfer to the hydroxyl group of serine or threonine residues in a protein to form GalNAc α1-O-serine/threonine. The GalNAc in the moiety of the GalNAc α1-O-serine/threonine is usually elongated and branched to give rise to a variety of complex O-GalNAc glycans in mammalian cells [2]. Indeed, hundreds of heterogeneous O-GalNAc glycans linked to serine/threonine have been found [1, 3]. To date, 20 isoforms of GALNTs have been identified in humans [4]; these are GALNT1-20, and evolutionarily conserved from unicellular eukaryotes to mammals [3].

High O-GalNAc glycan density influences the physical, chemical, and biological properties of mucin-type proteins [2]. Abnormalities in glycosylation are associated with various diseases. Although the causes of glycan abnormalities remain unclear, aging is thought to be a possible basis. Glycans change with aging, possibly affecting the onset or progression of age-related diseases, such as Parkinson's disease (PD) [3].

PD is conceptualized as a complex neurodegenerative disorder affecting approximately 6·1 million patients worldwide in 2016 [5–8]. Symptoms of PD are multifaceted. Patients with PD usually experience motor and non-motor symptoms. Current criteria define motor symptoms of PD patients as the presence of bradykinesia combined with resting tremors, rigidity, or both [5]. Additionally, non-motor symptoms include aspects of affects such as depression and anxiety, perception and thinking such as psychosis, and motivation such as impulse control disorders and apathy [6]. The duration of PD can span decades, and patients are commonly preceded by a potentially long prodromal period.

Although the etiology and pathology of PD remain unclear, considerable research has revealed that age is the most significant risk factor [7]. Since age also contributes to altered glycosylation, we sought to reveal an association between glycosylation and PD in this study.

Identifying and understanding glycosylation is critical for disease treatment and prevention; therefore, it is essential to explore the role of glycosyltransferases. GALNT9, UDP-GalNAc polypeptide N-acetylgalactosaminyltransferase 9, is a member of the GALNT family. GALNT9 expression has been reported in the brain [9]. However, the role of GALNT9 in PD has rarely been investigated. This study aimed to elucidate the critical role of GALNT9 in PD. Our goal was to improve the quality of life of PD patients by exploring the pathogenesis of PD related to glycosylation.

Methods and materials

Ethics approval of animal studies

This study was conducted in accordance with the principles of the Basel Declaration and the recommendations of the Dalian Medical University for laboratory animals. The study protocol was approved by the Animal Ethics Committee of Dalian Medical University.

Mice and mice treatments

C57BL/6J mice were used to generate a mouse model of PD-like variations. Male C57BL/6J mice (20–25 g) were obtained from the Laboratory Animal Center of the Dalian Medical University and were raised with unlimited access to food and water under specific pathogen-free conditions (temperature 22 ± 2 °C, humidity $55\pm5\%$).

In this study, a chronic PD-like phenotype was established in mice by intraperitoneal injection of 1-methyl-4-phenyl-1,2,3,6-tetrahydropyridine (MPTP), a neurotoxin. Ten-week-old mice (20–25 g) were randomly divided into two groups: a Control group and MPTP-treated cohort. Mice in the MPTP-treated group were administered an intraperitoneal injection of MPTP (25 mg/kg or 10 ml/kg, dissolved in physiological saline; Sigma-Aldrich, St. Louis, MO, USA) for 5 weeks at 3.5 day intervals. Mice in the Control group were intraperitoneally administered the same volume of physiological saline (10 ml/kg).

On the 1st and 3rd days after the last injection, behavioral assessments were performed using the pole and hanging tests. On the 7th day, all animals were sacrificed by cervical dislocation for confirmation of the model by detecting representative indices of PD, such as dopamine (DA) and tyrosine hydrolase (TH).

The apparatus for the pole test consisted of an iron pole (50 cm high, 0.5 cm diameter) that was wrapped with gauze to prevent slipping. The base of the pole was covered with bedding to protect mice from injury. Each mouse was positioned at the top of the pole facing upwards, and the total time for the mouse to turn around and climb down the pole from the top to the bottom was recorded. For the hanging test, the apparatus consisted of a narrow horizontal wire fixed between two vertical supports above the floor. Each mouse was positioned at the central point of the wire, and the latency for the mouse to hang-on to the wire was measured. Three trials, each with a one-hour interval, were conducted for each mouse.

Except for the evaluation of locomotor activity to identify the model mice, representative Parkinsonian indices were detected to confirm the model had PD-like variations. The detected indices included striatal DA and mesencephalic TH levels. Striatal DA was detected using reversed-phase high-performance liquid chromatography (RP-HPLC), and mesencephalic TH was examined using immunohistochemistry ().

Cell culture and treatment

Human SH-SY5Y neuroblastoma cells, an authenticated human dopaminergic neuronal cell line, were purchased from the Cell Bank of China (Shanghai, China). SH-SY5Y cells were cultured in Dulbecco's modified Eagle's medium (DMEM) supplemented with 10% fetal bovine serum and penicillin (100 units/mL)-streptomycin (100 µg/mL) at 37∘C under a 5% (v: v) CO_2 atmosphere.

For drug treatments, MPP$^+$ (1-Methyl-4-phenylpyridinium iodide, Sigma-Aldrich, St. Louis, MO, USA) was used to induce neuronal damage in this study. SH-SY5Y cells were seeded at 5×10^5 cells/mL and cultured to 70–80% confluence. Prior to the transfection of intervention plasmids, SH-SY5Y cells were incubated with 2.0 mM MPP$^+$ for 6 h at 37∘C.

Extraction of proteins and western blot

After the mice were sacrificed, the brains were separated and washed with ice-cold physiological saline (0.9%). The brain substructures, including midbrain, striatum, hippocampus, were carefully dissected, and each tissue was homogenized in RIPA (Radio Immunoprecipitation Assay) lysis buffer [pH 7.4, 50 mmol/L Tris with 150 mmol/L NaCl, 0.1% SDS, 1% sodium deoxycholate, 1% Triton X-100, and 1 mmol/L PMSF] (Phenylmethanesulfonyl fluoride) on ice. The protein lysates were cleared twice by centrifugation at 27,000 g for 30 min.

After trypsin digestion, SH-SY5Y cells were collected by centrifugation at 5000 g for 5 min. The collected SH-SY5Y cells were lysed by ultrasonication (5 s on, 3 s off), and the cell lysates were cleared by centrifugation at 27,000 g or 30 min twice.

Protein concentrations of the lysates were determined using the Bradford assay (Solabio, Beijing, China).

Twenty-five micrograms of total protein were separated by sodium dodecyl sulfate-polyacrylamide gel electrophoresis (SDS-PAGE). Proteins were transferred onto PVDF membranes after separation. Each membrane was blocked with 10% nonfat dry milk in Tris-buffered saline containing Tween-20 for 2 h at 25 ∘C. Next, the membranes were probed with primary antibodies overnight at 4 °C. The primary antibodies used in this study included monoclonal anti-GALNT9 (Thermo Fisher, Massachusetts, USA), anti-α-synuclein, anti-GAPDH (Abclone, Wuhan, China) and anti-TH (Abclone, Wuhan, China) antibodies, and polyclonal anti-Apaf1 (Huabio, China), anti-cytochrome C (CytC, Huabio, Hangzhou, China), anti-active caspase9 (CASP9, Huabio, Hangzhou, China) and anti-active caspase3 (CASP3, Huabio, Hangzhou, China) antibodies. The membranes were then incubated with a horseradish peroxidase-conjugated goat anti-mouse/rabbit secondary antibody for 45 min at room temperature. Protein bands were visualized using an enhanced chemiluminescent (ECL) system (GE Healthcare Bio-Sciences Corp.), and band densities were analyzed using ImageJ software.

Peng *et al. Biology Direct*   (2024) 19:77

Page 4 of 19

Immunohistochemistry (IHC) and immunofluorescent staining

Mice were anesthetized with diethyl ether and perfused with 0.9% physiological saline and 4% paraformaldehyde respectively. Following perfusion, the mouse brains were dehydrated across an increasing gradient of sucrose solutions including 15% and 30%, until the brain sank to the bottom in 30% sucrose solution at 4 °C. The mouse brains were embedded using OTC (optimal cutting temperature compound) in a cryostat, and the OTC-embedded frozen blocks were cut into 6–8 μm sections. Cryostat sections mounted on glass slides were used for further investigations, including IHC and immunofluorescent staining.

For IHC, the sections were permeabilized in 0.3% Triton X-100 in PBS (Phosphate Buffered Saline) for 20 min to increase penetration by the antibody, followed by incubation with 3% hydrogen peroxide for 10 min to eliminate endogenous peroxidase activity. Next, the sections were incubated in 5% bovine serum albumin in TBS (Tris-buffered saline) for 2 h at room temperature to block non-specific binding, followed by probing with specific primary antibodies at 4∘C overnight. The sections were then incubated with corresponding horseradish peroxidase-conjugated secondary antibodies for 1 h at room temperature and stained with 3,3'-diaminobenzidine (DAB) until a brown color appeared. Subsequently, the sections were counterstained with hematoxylin, dehydrated across an increasing ethanol gradient, including 75%, 85%, 95% 100% (twice) and xylene (3 times). Finally, IHC images were captured using a microscope. Additionally, the sections were washed with PBST (Phosphate Buffered Solution with Tween-20) (10 min × 3 times) every two steps.

For immunofluorescent staining, after permeation and blocking, the brain sections were probed with primary antibodies, followed by incubation with the corresponding secondary antibodies conjugated with Rhodopsin/FITC (Fluorescein isothiocyanate) for 1 h at room temperature in the dark. Next, brain sections were counterstained with DAPI (4,6-diamino-2-phenyl indole) to visualize nuclei. Images were acquired using a fluorescence microscope.

Construction, extraction, and transfection of pcDNA3.1-GALNT9 plasmid

Based on the sequence of *GALNT9* cDNA, a PCR primer pair used to amplify a *GALNT9* fragment was designed as *GALNT9*-F: *CTCGAG*ATGGCGGTGGCCAGGAAGATCCG (forward primer; the underlined section is a XhoI restriction endonuclease cleavage site) and *GALNT9*-R: *AAGCTT*TCAGTGCCGTGCGTGTTTGATCC (reverse primer; the underlined section is a HindIII site). The *GALNT9* fragment was amplified by PCR using a high-fidelity DNA polymerase. The purified *GALNT9*

PCR fragment was then cloned into plasmid pcDNA3.1, yielding pcDNA3.1-*GALNT9*, and DNA sequencing confirmation was performed.

Plasmids, including the constructed pcDNA3.1-*GALNT9* and the control pcDNA3.1, were extracted using an Endotoxin-Free Plasmid Extraction Kit. Afterwards, pcDNA3.1-*GALNT9* and pcDNA3.1 were transfected into SH-SY5Y cells using Lipofectamine™ 2000 (ThermoFisher Scientific, USA) at a 2:1 ratio (μl/μg, Lipofectamine 2000: nucleic acids = 2:1). SH-SY5Y cells harboring pcDNA3.1-*GALNT9*/pcDNA3.1 were cultured in an incubator with 5% CO_2 at 37∘C for 6 h. Then, the medium containing the transfection mixture was replaced with fresh medium containing 10% FBS, (fetal bovine serum) and the cells were cultured in an incubator under 5% CO_2 at 37℃ for a further 48 h.

Detection of apoptosis by annexin V and PI staining

Apoptosis was evaluated using the annexin V-fluorescein isothiocyanate (FITC)/propidium iodide (PI) Apoptosis Detection kit (Beyotime Biological Technology Research Institute, Shanghai, China). SH-SY5Y cells were seeded into 6-well plates and cultured for 48 h in an incubator at 37 °C with 95% humidity and 5% CO_2. The cells were then treated with MPP^+ and the corresponding plasmid, followed by incubation at 37 °C under 5% CO_2 for a further 24 h. Afterwards, the cells were incubated with 5 μL Annexin V and 4 μL of PI in the dark for 15 min at room temperature. Cells were analyzed by flow cytometry (Beckman Coulter Gallios) within 1 h, and apoptotic rates were quantified using FlowJo software.

Phalloidin staining for F-actin (a polymeric filament)

Actin is one of the most abundant and evolutionarily conserved proteins in eukaryotic cells. There are two forms of actin in cells: G-actin (monomeric form) and F-actin (polymeric filamentous state). Phalloidin, a bicyclic water-soluble heptapeptide isolated from *Amanita phalloides*, specifically recognizes F-actin. Therefore, in this study, the cellular cytoskeleton was evaluated based on detection of F-actin using phalloidin.

Coverslips were placed into 24-well plates and covered with 15 μL culture medium containing 10% FBS to prevent the coverslips from floating. SH-SY5Y cells were seeded into 24-well plates and cultured for 24 h in an incubator at 37 °C under 5% CO_2. Following treatment and incubation, SH-SY5Y cells were fixed with 4% paraformaldehyde for 40 min and permeabilized with 0.5% Triton X-100 in PBS for 20 min. Subsequently, the cells were incubated with FITC-labeled phalloidin working solution (v/v = 1:200, containing 1% BSA) at 37℃ for 30 min in the dark. Finally, the coverslips were counterstained with mounting medium containing 200 ng/mL

DAPI in PBS for 30 min in the dark, followed by image acquisition using a fluorescence microscope.

Evaluation of mitochondrial functions

Mitochondrial functions were measured by detecting ROS (Reactive Oxygen Specise) production and mitochondrial membrane potential (ΔΨm) which are related to energy generation, and mitochondrial permeability transition pores (mPTPs) and intracellular calcium concentration which are associated with mitochondrial inner-membrane permeability. The final image acquisition of the assays, including ΔΨm and calcium ions, were performed using flow cytometry. For mPTP and ROS assays, fluorescent signals were photographed using a fluorescence microscope. Thus, for assays of ΔΨm and calcium, cells were seeded into 6-well plates, whereas for assays of mPTPs and ROS, the cells were seeded into 24-well plates with coverslips. Following treatment and incubation, SH-SY5Y cells were stained with fluorescent probes.

Measurements of ΔΨ were performed using a JC-1 probe (Beyotime Biological Technology Research Institute, Shanghai, China). SH-SY5Y cells were incubated with JC-1 probe in serum-free culture medium (1:10 dilution) at 37 °C for 20 min. After measurement by flow cytometry, the percentage of cells with fluorescent signals was calculated.

ROS levels were determined using the fluorogenic dye probe, 2,7-dichlorodihydrofluorescein diacetate (DCFH-DA). SH-SY5Y cells on coverslips were incubated with DCFH-DA probe at 37 °C for 20 min in the dark. Fluorescence signals were photographed using a fluorescence microscope (excitation, 488 nm; emission, 510–530 nm).

mPTP opening was evaluated using calcein-acetoxymethyl ester (calcein-AM)/cobalt (Beyotime Biological Technology Research Institute, Shanghai, China). SH-SY5Y cells on coverslips were incubated with calcein-AM (1 μM) and $CoCl_2$ (5 μM) solution at 37 °C for 30 min. Then, the dye solution was replaced by pre-warmed DMEM medium containing 10% FBS. The cells were then incubated at 37 °C for 30 min. Finally, fluorescence signals were imaged using a fluorescence microscope.

Intracellular calcium content was determined using the fluorogenic dye Fluo-4 AM. SH-SY5Y cells were incubated with Fluo-4 AM solution at 37 °C for 60 min. Fluorescence signals were analyzed by flow cytometry, and data are presented as the percentage of cells with fluorescence signals.

Determination of mitophagy

SH-SY5Y cells on coverslips were fixed and permeabilized, followed by incubation with pre-warmed Mito-Tracker® Red and CMXRos dyes (200 nM, Solarbio) which specifically stain mitochondria, and LysoTracker Green DND-26 solution (75 nM, Solarbio) which specifically stains lysosomes. Fluorescent signals were acquired using a fluorescence microscope.

Statistical analysis

Statistical analyses were performed using GraphPad Prism 9 software (GraphPad Software, Inc., La Jolla, CA, USA). One-way analysis of variance (ANOVA) was used to compare data. Quantitative data are presented as means±standard error of the mean (SEM), and $P < 0.05$ was considered statistically significant.

Results and discussion

Low GALNT9 and O-GalNAc glycosylation levels in brains of MPTP-treated mice

GALNT9 is expressed specifically in the brain [9]. Theoretically, GALNT9 plays important roles in the regulation of brain functions. In this study, to determine whether GALNT9 or its catalytic products are associated with PD, we evaluated glycosylation levels of GALNT9 and its catalytic product, protein O-GalNAc, in mouse brains. Consequently, universally downregulated GALNT9 was found in the brains of mice with PD-like variations. As shown in Fig. 1B and D, GALNT9 exhibited tissue-specific expression in different structures of the mouse brain, including the midbrain, striatum, and hippocampus. In fact, a significant decrease in soluble GALNT9 was detected in midbrain structures (Control: 1.419±0.306; MPTP-treated: 1.008±0.103; $P=0.006$), striatum (Control: 0.807±0.225; MPTP-treated: 0.447±0.208; $P=0.009$), and hippocampus (Control: 1.784±1.095; MPTP-treated: 0.749±0.125; $P=0.029$) in MPTP-treated mice. Thus, low levels of GALNT9 are associated with PD-like variations.

GALNT9 initiates O-GalNAc glycosylation of proteins, and the catalytic product of the first alpha-GalNAc can be specifically recognized by Dolichos Biflorus Agglutinin (DBA). Therefore, biotin-labeled DBA was used to detect O-GalNAc glycosylation. As illustrated in Fig. 1A, C and a dramatic reduction in protein O-GalNAc glycosylation was observed in MPTP-treated mice compared to controls. For the detected special structures, including midbrain (Control: 3.548±0.373; MPTP-treated: 2.118±0.928; $P=0.002$), striatum (Control: 3.265±0.723; MPTP-treated: 2.245±0.980; $P=0.027$), and hippocampus (Control: 3.150±0.279; MPTP-treated: 2.020±1.171; $P=0.013$), all showed a decrease in protein O-GalNAc glycosylation.

Western blot analysis revealed a reduction in soluble GALNT9 and its catalytic products for protein O-GalNAc glycosylation in MPTP-treated mice relative to controls. As previously reported, GALNT9 is specifically expressed in the brain; therefore, protein O-GalNAc glycosylation catalyzed by GALNT9 may play a role in the
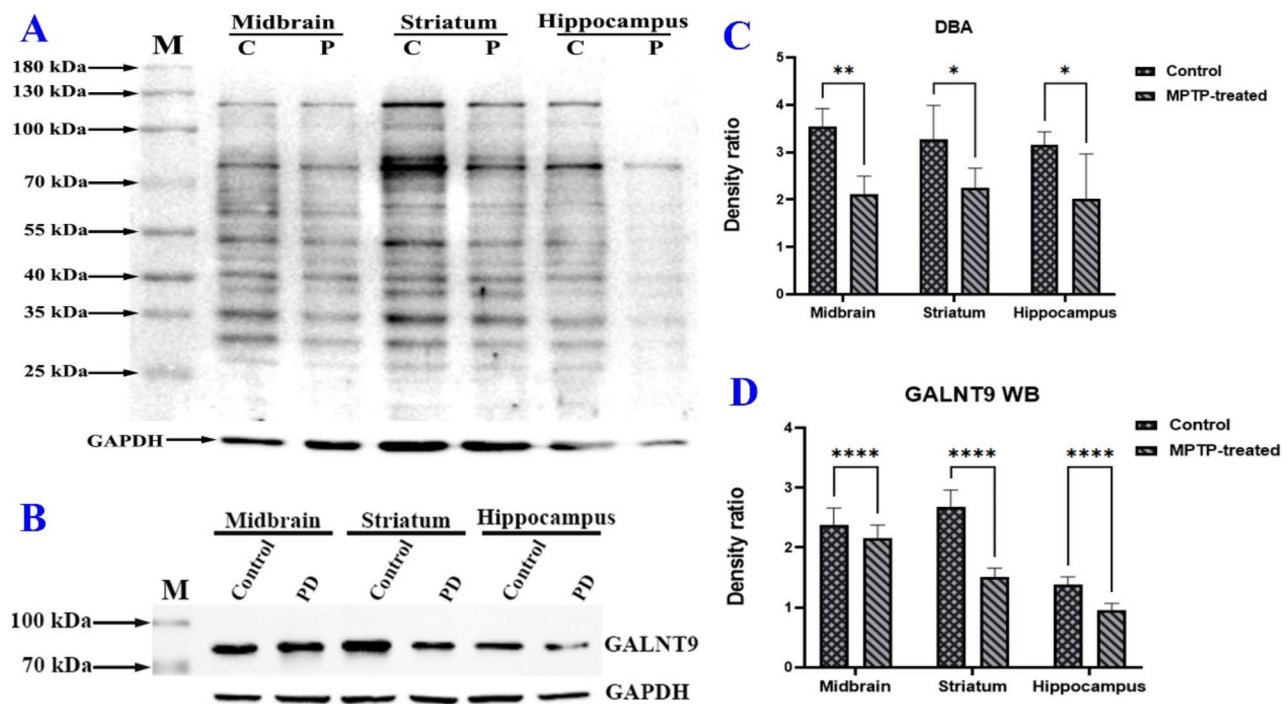
Fig. 1 Evaluation of levels of GALNT9 and its catalytic products by western blot assay. Examinations were performed in triplicate at least. M, PageRuler prestained protein ladder (Fermentas); *, $P < 0.05$; **, $P < 0.01$; ***, $P < 0.001$. (**A**) Representative images illustrating levels of DBA-recognized proteins. The probe was biotinylated DBA. (**B**) Representative images illustrating GALNT9 expression. The probe was a monoclonal anti-GALNT9 antibody. (**C**) Statistical analysis of DBA-recognized proteins normalized to GAPDH abundance. (**D**) Statistical analysis of soluble GALNT9 normalized to GAPDH levels

brain. Additionally, although the first GalNAc linked to a protein can be elongated and branched, the DBA-recognized moiety indicates the level of protein O-GalNAc glycosylation to some extent.

Our study showed that levels of both soluble GALNT9 and its catalytic products were decreased in mice with PD-like variations, especially in the midbrain, striatum, and hippocampus. Thus, low levels of GALNT9- or DBA-recognized proteins are highly suspected to be associated with PD-like variations. In fact, our most recent published study revealed low levels of plasma GALNT9 in patients with PD by testing clinical samples using qPCR assays [10]. The detection of plasma GALNT9 levels confirmed that low levels of GALNT9 are potentially related to PD.

Efficient GALNT9 up-regulation in neuroblastoma cells harboring pcDNA3.1-GALNT9 plasmid

In this study, SH-SY5Y cells were treated with MPP+, an active form of MPTP, to induce Parkinsonian variations in vivo. In vitro evaluation of cellular GALNT9 levels showed that GALNT9 was dramatically downregulated following MPP+ exposure (Fig. 2C and D). Consistent with cellular GALNT9 levels, cells treated with MPP+ exhibited significantly decreased levels of DBA-recognized proteins (Fig. 2A and B). Taken together, a

deficiency in soluble GALNT9 was found in the brains of mice with PD-like variations and in cells treated with MPP+. In addition, levels of GALNT9 catalytic products were significantly downregulated in MPP+-and MPTP-induced mice.

Because a low level of GALNT9 was associated with PD-like variations, we constructed a plasmid overexpressing GALNT9 to determine whether GALNT9 supplementation plays a role in ameliorating the cytotoxicity of PD-like variations. The neuroblastoma cell line SH-SY5Y was used in this study, and a cell model with GALNT9 supplementation was achieved by introducing the recombinant pcDNA3.1-*GALNT9* plasmid into SH-SY5Y cells.

Based on the above evidence, we introduced a plasmid that can overexpress GALNT9 in neuroblastoma cells to investigate the influence of GALNT9 abundance on neuronal cells. Based on the *GALNT9* sequence, a recombinant plasmid containing *GALNT9* (pcDNA3.1-*GALNT9*) was constructed and confirmed by digestion with restriction endonucleases XhoI and HindIII (Fig. 2E), followed by confirmatory DNA sequencing. The effect of pcDNA3.1-*GALNT9* on neuronal cells was determined using western blotting. Figure 2F and G show that recombinant plasmid containing *GALNT9* significantly facilitated GALNT9 expression in SH-SY5Y
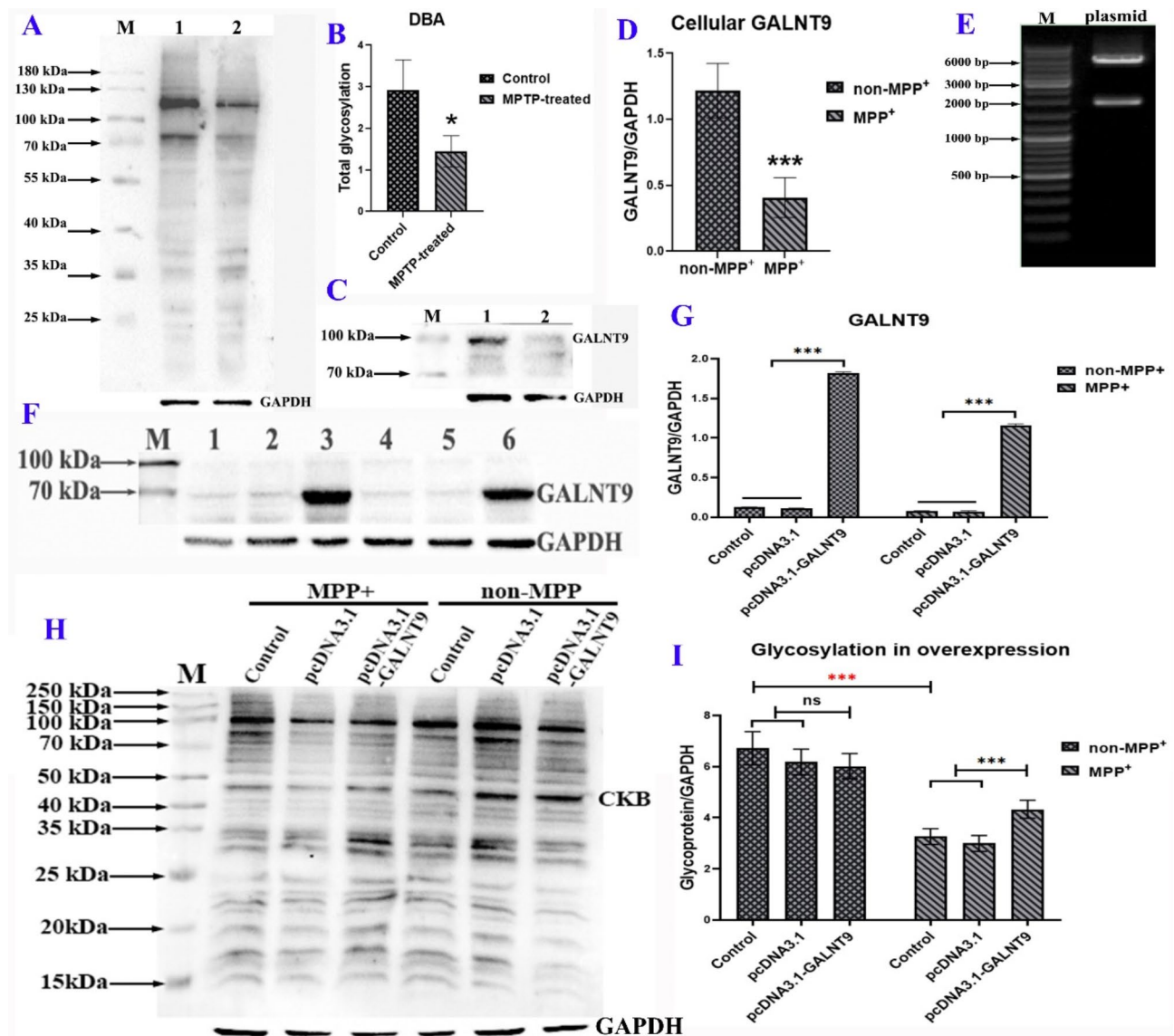
Fig. 2 Identification of overexpressed GALNT9 in SH-SY5Y cells. Examinations were performed in triplicate at least. M, PageRuler prestained protein ladder (Fermentas). *, $P < 0.05$; **, $P < 0.01$; ***, $P < 0.001$. (**A**) Representative images illustrating cellular glycoproteins with GalNAc moiety by western blot assays. The probe was biotinylated DBA. (**B**) Statistical analysis of cellular glycoproteins with GalNAc moiety normalized to GAPDH levels. (**C**) Representative images illustrating GALNT9 expression by western blot assays. The probe was anti-GALNT9 monoclonal antibody. (**D**) Statistical analysis of GALNT9 normalized to GAPDH abundance. (**E**) Identification of plasmid pcDNA3.1-*GALNT9*. The plasmid was digested with XhoI and HindIII. (**F**) Abundance analysis of GALNT9 in SH-SY5Y cells. The probe was anti-GALNT9 monoclonal antibody. (**G**) Statistical analysis of GALNT9 abundance in SH-SY5Y cells normalized to GAPDH levels. (**H**) Abundance analysis of glycoproteins with GalNAc moiety in SH-SY5Y cells. The probe was biotin-labeled DBA. (**I**) Statistical analysis of glycoproteins with GalNAc moiety in SH-SY5Y cells normalized to GAPDH levels

cells. Additionally, glycosylation analysis revealed that MPP$^+$ treatment directly led to reduced glycosylation, as detected by biotinylated DBA (Fig. 2A and B), whereas pcDNA3.1-*GALNT9* dramatically enhanced the total levels of glycoproteins with the GalNAc moiety in MPP$^+$-treated cells compared to controls (Fig. 2H and I). This suggests that the abundance of DBA-recognized proteins is potentially influenced by GALNT9.

Thus, a cell model harboring overexpressed GALNT9 was established using neuroblastoma SH-SY5Y cells in this study, which was applicable for subsequent analyses of the effects of GALNT9 enrichment on cell fate.

GALNT9 enrichment ameliorated MPP+-induced cytotoxicity

Thyroid hydroxylase (TH) and DA are representative parameters used to assess PD patients. Thus, we evaluated the levels of these indices (TH and DA) to measure the effect of GALNT9 on cytotoxicity, which causes PD-like variations.

TH: Soluble TH was detected by western blotting. As displayed in Fig. 3A, B and a significant decrease in TH levels occurred in MPP$^+$-treated cells relative to the non-MPP$^+$-treated SH-SY5Y cells (non-MPP$^+$: 1.223±0.248; MPP$^+$: 0.385±0.075; $P < 0.001$). Under MPP$^+$ conditions, GALNT9 enrichment dramatically increased TH levels compared to control cells (pcDNA3.1/MPP$^+$: 0.362±0.063; GALNT9/MPP$^+$: 0.821±0.236; $P < 0.001$) (Fig. 3A and B).

DA: DA analysis was performed using HPLC. As illustrated in Fig. 3C, MPP$^+$ treatment resulted in a dramatic reduction in intracellular DA content (non-MPP$^+$: 116.502±9.951; MPP$^+$: 51.583±18.640; $P < 0.001$). Under MPP$^+$ exposure, GALNT9 enrichment significantly increased DA levels (pcDNA3.1/MPP$^+$: 55.816±5.333; GALNT9/MPP$^+$: 84.589±10.709; $P < 0.001$) in SH-SY5Y cells (Fig. 3C).

Apoptosis cell apoptosis assays were performed using the Annexin V-FITC (Fluorescein isothiocyanate)/PI (propidium iodide) apoptosis detection kit (Beyotime Biotechnology, Shanghai, China), and apoptotic rates were calculated based on the sum of the late and early apoptotic rates. As shown in Fig. 3D, MPP$^+$ treatment (28.720±1.828%) significantly enhanced cell apoptosis compared to untreated cells (17.590±1.489%), thus excessive apoptosis might lead to cell death. Upon exposure to MPP$^+$, GALNT9 supplementation ameliorated the high apoptotic rates induced by MPP$^+$ to a reasonable level (20.700±3.918%), which was similar to that observed in non-MPP$^+$-treated cells).

Taken together, MPP$^+$ treatment directly induced cytotoxicity in SH-SY5Y cells. Based on low levels of cellular TH and DA and a high rate of apoptosis, SH-SY5Y cells under MPP$^+$ exposure were expected to show cytotoxicity similar to PD. However, GALNT9 supplementation showed an activity in ameliorating cytotoxicity induced by MPP$^+$, as it greatly increased the levels of cellular TH and DA, and significantly decreased apoptotic rates. These results imply that GALNT9 enrichment significantly ameliorated the cytotoxicity induced by MPP$^+$ by enhancing levels of intracellular DA and TH and reducing excessive apoptosis.
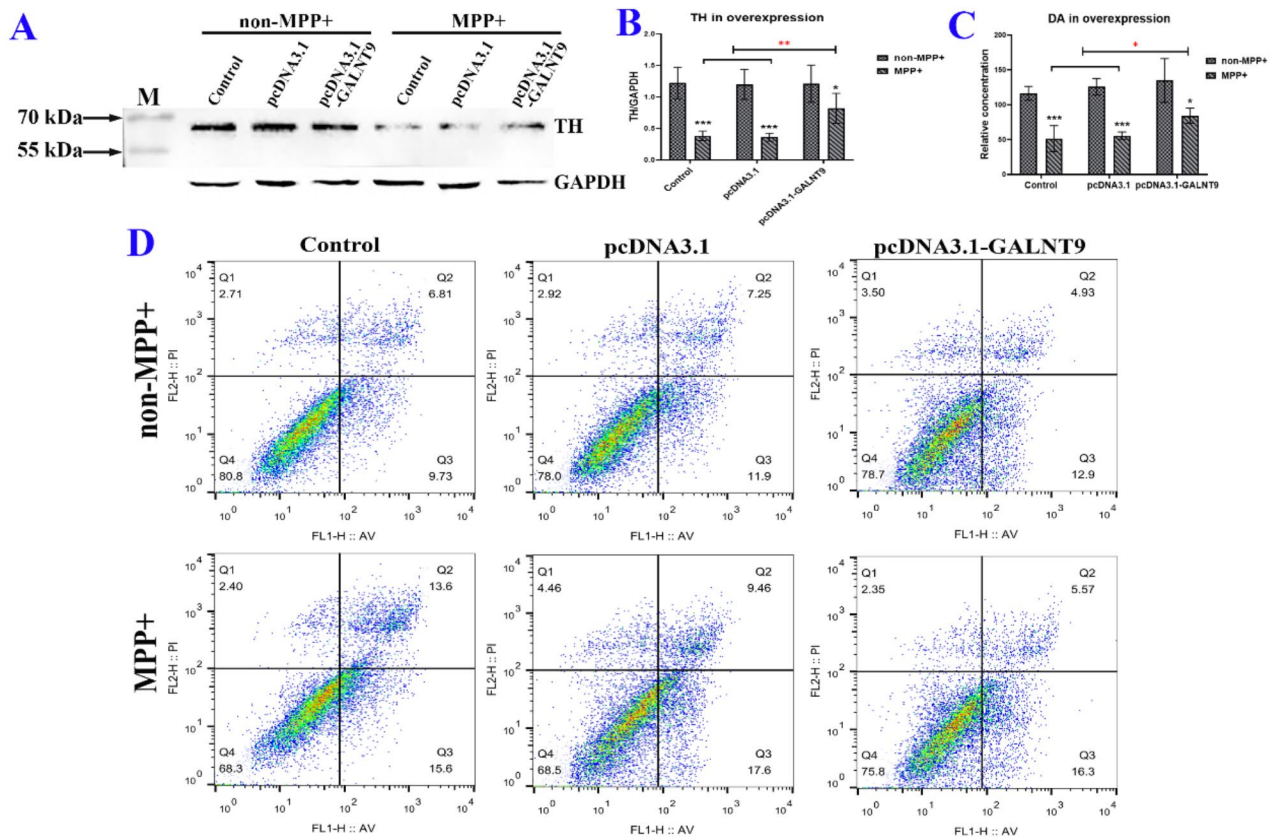

Fig. 3 Influence of GALNT9 on cytotoxicity in SH-SY5Y cells. Examinations were performed in triplicate at least. M, PageRuler prestained protein ladder (Fermentas); Black asterisks represent comparison between MPP$^+$-treated and untreated groups; Red asterisks indicate comparison between GALNT9-related groups and controls. *, $P < 0.05$; **, $P < 0.01$; ***, $P < 0.001$. (**A**) Abundance analysis of TH in SH-SY5Y cells using western blot assays. Polyclonal anti-TH antibody was used as a probe. (**B**) Statistical analysis of intracellular TH levels in SH-SY5Y cells. (**C**) Statistical analysis of intracellular DA abundance in SH-SY5Y cells. (**D**) Apoptosis analysis of SH-SY5Y cells using an Annexin V-FITC/PI apoptosis detection kit
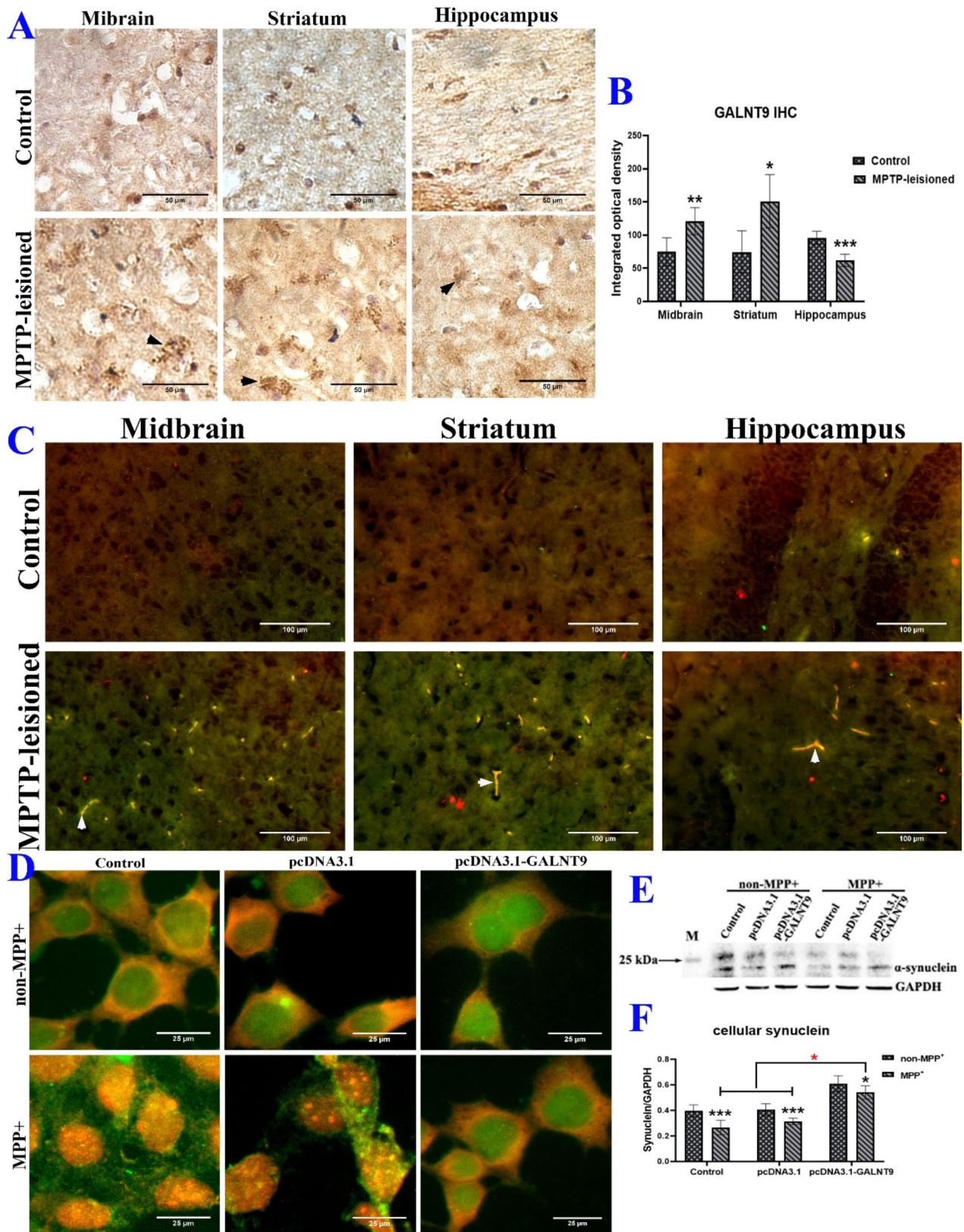
Fig. 4 (See legend on next page.)

(See figure on previous page.)

Fig. 4 Influence of GALNT9 on protein aggregates containing DBA-recognized proteins and α-synuclein. Examinations were performed in triplicate at least. *, $P < 0.05$; **, $P < 0.01$; ***, $P < 0.001$. (**A**) Analysis of total GALNT9 using IHC assays. An anti-GALNT9 monoclonal antibody was used as the probe. The black arrows indicate GALNT9 in glial cells. The micrograph was 558.8 mm × 558.8 mm (**B**) Statistical analysis of total GALNT9 detected by IHC. (**C**) Dual immunofluorescence staining of DBA-recognized glycoproteins with α-synuclein in vivo. The micrograph was 1731.43 mm × 1151.47 mm. Red signals corresponded to DBA-recognized glycoproteins. Green signals corresponded to α-synuclein. Colocalization of DBA-recognized glycoproteins with α-synuclein is depicted as the juxtaposed images in green and red. Dual immunolabelling of DBA-recognized glycoproteins/α-synuclein visible as bright orange or yellow indicated by white tips. (**D**) Dual immunofluorescence staining of DBA-recognized glycoproteins with α-synuclein in vitro. The micrograph was 357.72 mm × 357.72 mm (**E**) Abundance analysis of cellular α-synuclein by western blot assay. The probe was a monoclonal antibody against α-synuclein. M, PageRuler prestained protein ladder (Fermentas). (**F**) Statistical analysis of soluble α-synuclein levels

GALNT9 enrichment ameliorated α-synuclein-containing protein aggregations

Low levels of soluble GALNT9 were detected in the brains of MPTP-treated mice using an immunostaining assay. However, the IHC assay for GALNT9 displayed the opposite abundance levels in the midbrain and striatum, as shown in Fig. 4A and B, with the exception of the hippocampus. A low level of hippocampal GALNT9, which was consistent with the results obtained by immunostaining, was observed in MPTP-treated mice relative to control mice. However, Fig. 4A illustrates that the midbrain and striatum exhibited strong immunoreactivity toward α-synuclein ($P < 0.05$) in MPTP-treated mice. Statistical analysis revealed higher levels of mesencephalic and striatal GALNT9 in MPTP-treated mice than in control mice.

Thus, the results from IHC assays were contrary to those from western blot analyses of the midbrain and striatum. Usually, IHC assays evaluate total GALNT9, whereas western blotting assesses soluble GALNT9 levels. This suggests that the downregulation of soluble GALNT9 possibly results from protein deposition containing GALNT9 in insoluble forms, further leading to decreased levels of catalytic products of glycoproteins with O-GlaNAc.

In addition, microscopy (Fig. 4A) revealed that hundreds of scattered and dot-like dark-stained GALNT9 spots were clustered together only in the brains of MPTP-treated mice, in the midbrain, striatum, or hippocampus, although a low level of hippocampal GALNT9 was detected in MPTP-treated mice. In fact, this evidence potentially shows that GALNT9 was redistributed in the brains of MPTP-treated mice compared to controls. Coupled with low levels of soluble GALNT9, which were detected by western blotting, this suggested that GALNT9 was possibly deposited and redistributed in an insoluble form to lower its soluble form in the brains of MPTP-treated mice.

Furthermore, a report by the group of Nakamura et al. demonstrated GALNT9 expression in hippocampus using in situ hybridization (ISH) in 2005. Based on ISH images, Nakamura interpreted large, intensely stained spots as neurons and small, intensely stained spots as glial cells [11]. In this study, we identified GALNT9 distribution using IHC assays. According to Nakamura's

description, we assumed that GALNT9 was intensely expressed in neurons, but not glial cells, under physiological conditions; however, the expression of GALNT9 in glial cells was greatly increased under pathological conditions. These data are consistent with those reported by Nakamura et al. Therefore, glial GALNT9 is suspected to be exclusively associated with the pathogenesis of PD.

The neuropathological hallmark of PD is neuronal protein aggregates, termed Lewy bodies [12], which are intracytoplasmic inclusion bodies composed largely of intermediate filament proteins [13]. In particular, of the proteins involved, misfolded and aggregated α-synuclein is considered to be the main component of Lewy bodies [14].

As GALNT9 catalyzes the initial step in linking GalNAc to serine/threonine residues of proteins, glycoproteins with the initial O-GalNAc are potentially the catalytic products of GALNT9. Thereby, this study investigated protein aggregates containing α-synuclein and glycoproteins using a monoclonal anti-α-synuclein antibody and biotinylated Dolichos Biflorus Agglutinin (DBA) as probes, respectively. DBA has N-acetylgalactosamine carbohydrate specificity. Although DBA cannot recognize all GALNT9 catalytic products owing to further glycosylation by extending the O-GalNAc moiety, DBA-recognized proteins can indicate the activity of GALNT9 to some extent (Fig. 2H and I).

As shown in Fig. 4C, protein aggregates containing α-synuclein and DBA-recognized glycoproteins were investigated. In the micrographs, DBA-recognized protein is shown in red, and α-synuclein is indicated in green. The channel overlaps, depicted as bright orange or yellow, were detected using ImageJ software. In this study, bright yellow- or orange-colored spots represent the localization of protein aggregations formed by DBA-recognized proteins and α-synuclein. Multiple colored spots were found in micrographs of MPTP-treated brains compared to controls (Fig. 4C). Interestingly, rod-shaped spots with bamboo-like joints were observed in the midbrain, striatum, and hippocampus. These strong yellow or orange signals indicated that protein aggregates containing DBA-recognized protein and α-synuclein were specifically located in the brains of mice with PD-like variations. Therefore, DBA-recognized proteins may be potential components of Lewy bodies by interacting with

α-synuclein, further contributing to the pathogenesis of PD.

In vitro assays employing dual immunofluorescent staining of glycoprotein and α-synuclein also showed that co-localization of DBA-recognized proteins and α-synuclein were only detected in MPP⁺-induced cells (Fig. 4D). As shown in Fig. 4D, a large yellow/orange overlap was visible in the two MPP⁺-treated groups (control/MPP⁺ and pcDNA3.1/MPP⁺). However, GALNT9 enrichment significantly attenuated this color overlap induced by MPP⁺. Thus, these findings demonstrated that GALNT9 enrichment efficiently reduced the formation of protein aggregations containing DBA-recognized proteins and α-synuclein under MPP⁺ exposure (Fig. 4D), and significantly increased soluble α-synuclein levels in MPP⁺-induced cells (Fig. 4E and F). This indicates that glycoproteins with abnormal O-GalNAc levels are involved in the formation of protein aggregates containing α-synuclein.

Taken together, these findings indicate that low levels of GALNT9 possibly resulted from its deposition and redistribution in an insoluble form, which led to decreased protein glycosylation. Glycoproteins with insufficient glycosylation modifications were associated with protein inclusions via interaction with α-synuclein. Formation of protein aggregates by DBA-recognized proteins and α-synuclein under MPP⁺ exposure was ameliorated by increasing GALNT9 levels. Furthermore, another possibility is that down-regulated GALNT9 resulted from the conversion of neuronal GALNT9 into glial GALNT9, and that glial GALNT9 was associated with the pathogenesis of PD.

Positive regulation of mitochondrial energy generation with GALNT9 enrichment

ΔΨm

Nowadays, the involvement of mitochondria in the pathogenesis of PD is of great concern globally. Mitochondria are the powerhouses for cellular energy generation and produce ATP via oxidative phosphorylation coupled with an electron transport chain [15]. In the electron transport chain, a proton gradient in terms of trans-membrane potential (ΔΨm), is generated across the inner-membrane of mitochondria, and drives ATP to be produced by mitochondria. Usually, ΔΨm levels remain dynamically stable in cells under physiological conditions.

Due to the important implications of ΔΨm for energy generation, we measured ΔΨm using a fluorescent JC-1 probe coupled with flow cytometry in this study. Green fluorescence indicated a low level of ΔΨm. In this study, rates of cells with green fluorescence signals were statistically calculated using cytometric images. As illustrated in Fig. 5B, MPP⁺ exposure (59.700±3.466%)

resulted in a dramatic increase in the percentage of cells with green fluorescence signals relative to untreated cells (43.200±1.411%). With MPP⁺ exposure, GALNT9 enrichment (39.267±6.207%) largely decreased the percentage of cells with low membrane potential compared to control cells harboring pcDNA3.1 plasmid only (59.667±2.854%). In fact, a limited fluctuation in ΔΨm is necessary for healthy mitochondrial functioning, since ΔΨm is involved in maintaining mitochondrial homeostasis via selective elimination of malfunctional mitochondria. However, a sustained drop or rise in ΔΨm is deleterious for cells. Our study showed that MPP⁺ exposure caused a sustained drop in ΔΨm, leading to dysfunction of mitochondria in bioenergetic generation. However, GALNT9 enrichment ameliorated this sustained drop in ΔΨm induced by MPP⁺. Therefore, we elucidated a protective role of GALNT9 enrichment in cellular energy generation.

ROS

Reactive oxygen species (ROS) are implicated in aging and many neurodegenerative pathologies [16, 17], and are formed as byproducts of energy generation. Usually, a significant increase in ROS levels results from abnormal levels of ΔΨm across the inner mitochondrial membrane. As noted, cells with PD-like cytotoxicity exhibit a high percentage of cells with abnormal ΔΨm, so we investigated cellular ROS levels using the fluorogenic dye DCFH-DA in this study. Bright green spots indicate ROS. As illustrated in Fig. 5A, considerable ROS accumulation was detected in MPP⁺-treated cells compared to that in untreated cells. However, GALNT9 enrichment significantly reduced the excessive ROS production induced by MPP⁺. This finding regarding ROS accumulation was consistent with ΔΨm measurements.

Thus, GALNT9 enrichment facilitated mitochondrial metabolic function in energy generation through attenuating ROS levels and ameliorating aberrant ΔΨm.

Actin cytoskeleton

As noted, GALNT9 has a role in ameliorating bioenergetic failure induced by MPP⁺ treatment via attenuating ROS accumulation and aberrant ΔΨm. In this study, the influence of GALNT9 on energy generation was verified by evaluating the integrity of the actin cytoskeleton, a complex of actin filaments organized into diverse structural arrays by numerous regulatory and accessory proteins [18]. Actin filaments (F-actin) are critical for eukaryotic cell migration, shape, mechanical integrity, polarity, and transcriptional regulation [19]. F-actin is comprised of linearly polymerized monomeric globular actin (G-actin) [20], which contains a single polypeptide chain with bound adenine nucleotides in cells [21]. Dynamic polymerization of the actin cytoskeleton is an
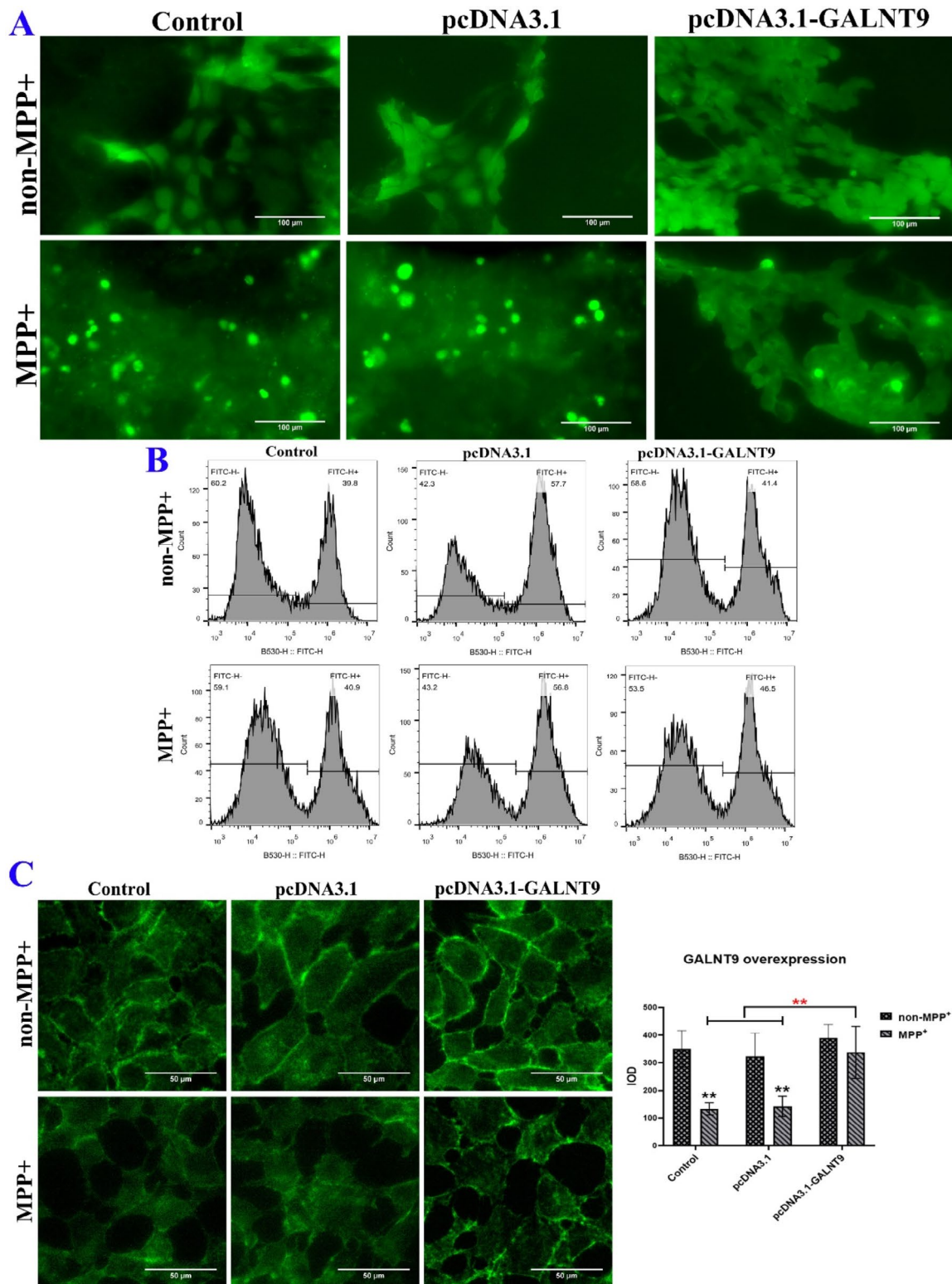
Fig. 5 Influence of GALNT9 on energy generation. Examinations were performed in triplicate at least. (**A**) Representative micrographs of intracellular ROS determined by fluorescence microscopy. The images were 1731.43 mm × 1151.47 mm. Bright green signals represent positive areas of ROS. (**B**) Evaluation of ΔΨm by flow cytometry. JC-1 staining was used. The rates of FITC-positive cells were calculated to indicate a low ΔΨm. (**C**) Representative micrographs of cytoskeletal actin filaments and statistical analysis of fluorescence intensity. The dimension of micrographs was 529.17 mm × 529.17 mm. The cytoskeleton was stained with FITC-phalloidin (green), and images were captured using fluorescence a microscope. *, $P < 0.05$; **, $P < 0.01$; ***, $P < 0.001$

ATP-dependent process [22]. Collective studies have indicated that approximately 50% of the total ATP in a cell is required to support cytoskeletal actin rearrangement [19]. For example, it is reported the assembly of the actin cytoskeleton consumes up to 50% of total ATP in resting platelets [23].

Therefore, integrity of the actin cytoskeleton was evaluated by measuring levels of ATP generated using FITC-labeled phalloidin staining. As shown in Fig. 5C, fluorescent signals were clearly visible in the non-MPP+ groups, including the control, pcDNA3.1, and pcDNA3.1-*GALNT9* cohorts. However, statistical analysis revealed that MPP+ caused a massive loss in the intensity of fluorescent signals with respect to controls (Control/non-MPP+: 267.577 ± 32.971; Control/MPP+: 173.168 ± 50.114; $P=0.029$). Upon MPP+ exposure, dramatic increases in filament bundles and enhanced barbed ends were evident in cells overexpressing GALNT9 as determined by fluorescence microscopy. Thus, FITC-labeled phalloidin staining supported that GALNT9 plays a role in enhancing the synthesis of actin filaments in the cytoskeleton. Consistent with the roles in energy generation regulated by GALNT9, GALNT9 supplementation led to greater stiffness of the cytoskeletal network, signifying that sufficient ATP was supplied for actin cytoskeletal rearrangement when GALNT9 was overexpressed in cells.

Thereby, based on these observations, we assumed that GALNT9 enrichment raises the level of energy generation by ameliorating aberrant $\Delta\Psi m$ and reducing ROS levels, leading to sufficient ATP supply for dynamic assembly of actin cytoskeletal components.

GALNT9 enrichment ameliorated abnormal mitochondrial membrane permeability induced by MPP+

Mitochondria allow Ca^{2+} release and/or metabolite exchange between the mitochondrial matrix and cytosol, with an exclusion size of 1,500 Da, via mPTPs, nonspecific channels within the inner mitochondrial membrane. This increased permeability of mPTPs can be triggered by various pathological and physiological stimuli. The long-lasting opening of mPTPs results in rupture of the outer mitochondrial membrane (OMM), collapse of $\Delta\Psi m$, and cessation of ATP synthesis, ultimately leading to necrotic cell death [24–26]. Prolonged opening of mPTPs is detrimental to cells and is associated with pathological conditions such as neurodegenerative diseases.

mPTPs

In this study, mitochondrial membrane permeability was assessed using a calcein-AM (Acetoxymethyl Ester)/cobalt assay. Because mitochondria tend to cluster along the plasma membrane, a marked circular distribution of bright green fluorescent signals indicates that the mPTPs are in a closed configuration. As

shown in Fig. 6A, marked circular fluorescent signals were evident in the non-MPP+-treated cells harboring pcDNA3.1, pcDNA3.1-*GALNT9*, and the control, as well as in MPP+-treated cells harboring pcDNA3.1-*GALNT9*, although the fluorescence intensities of calcein in the MPP+-treated cells harboring pcDNA3.1-*GALNT9* were not as strong as those in non-MPP+-treated cells. However, no clear circular fluorescence signals were observed in the two MPP+-treated cell lines without GALNT9 overexpression. This suggests that MPP+ treatment led to a massive loss of calcein fluorescence in cells, signifying mPTPs opening, whereas GALNT9 enrichment ameliorated the MPP+-induced open configuration of mPTPs. These findings indicate that GALNT9 is highly active in regulating mPTPs opening. GALNT9 enrichment confers protection against prolonged mPTPs opening.

Ca2+

In neurons, intracellular calcium is involved in regulating an array of cellular processes and is crucial for signal transduction. Once calcium enters neurons, it is rapidly sequestered by sub-organelles such as the mitochondria and endoplasmic reticulum (ER) [27]. It is fundamental that mitochondria are able to accumulate, retain, and release intracellular calcium [27]. It has been reported that accumulation of intracellular calcium in mitochondria triggers activation of oxidative phosphorylation and a subsequent increase in ATP generation [28]. Calcium sequestered in the mitochondria can be pumped back into the cytosol via channels or transporters. In fact, mPTPs mediate calcium efflux. In this study, we evaluated calcium release to measure mitochondrial membrane permeability using a Fluo-4 AM probe coupled with flow cytometry. Flow cytometry data were expressed as the percentage of cells with fluorescent signals. As shown in Fig. 6B, the fluorescence intensity in cells under MPP+ exposure ($59.923 \pm 2.052\%$) was dramatically augmented compared to untreated cells ($53.755 \pm 1.075\%$). Under MPP+-treated conditions, GALNT9 enrichment ($53.113 \pm 1.314\%$) reduced the leakage of Ca^{2+}. These results indicate that GALNT9 enrichment inhibited calcium efflux. This finding demonstrated that GALNT9 influences mitochondrial permeability and that GALNT9 enrichment ameliorated prolonged mPTP opening and reduced Ca^{2+} release. Based on these findings, we hypothesized that GALNT9 enrichment might reduce calcium efflux by ameliorating prolonged mPTP opening.

This further confirmed that GALNT9 enrichment ameliorated the increase in non-specific mitochondrial permeability and maintained mitochondria in a healthy state.
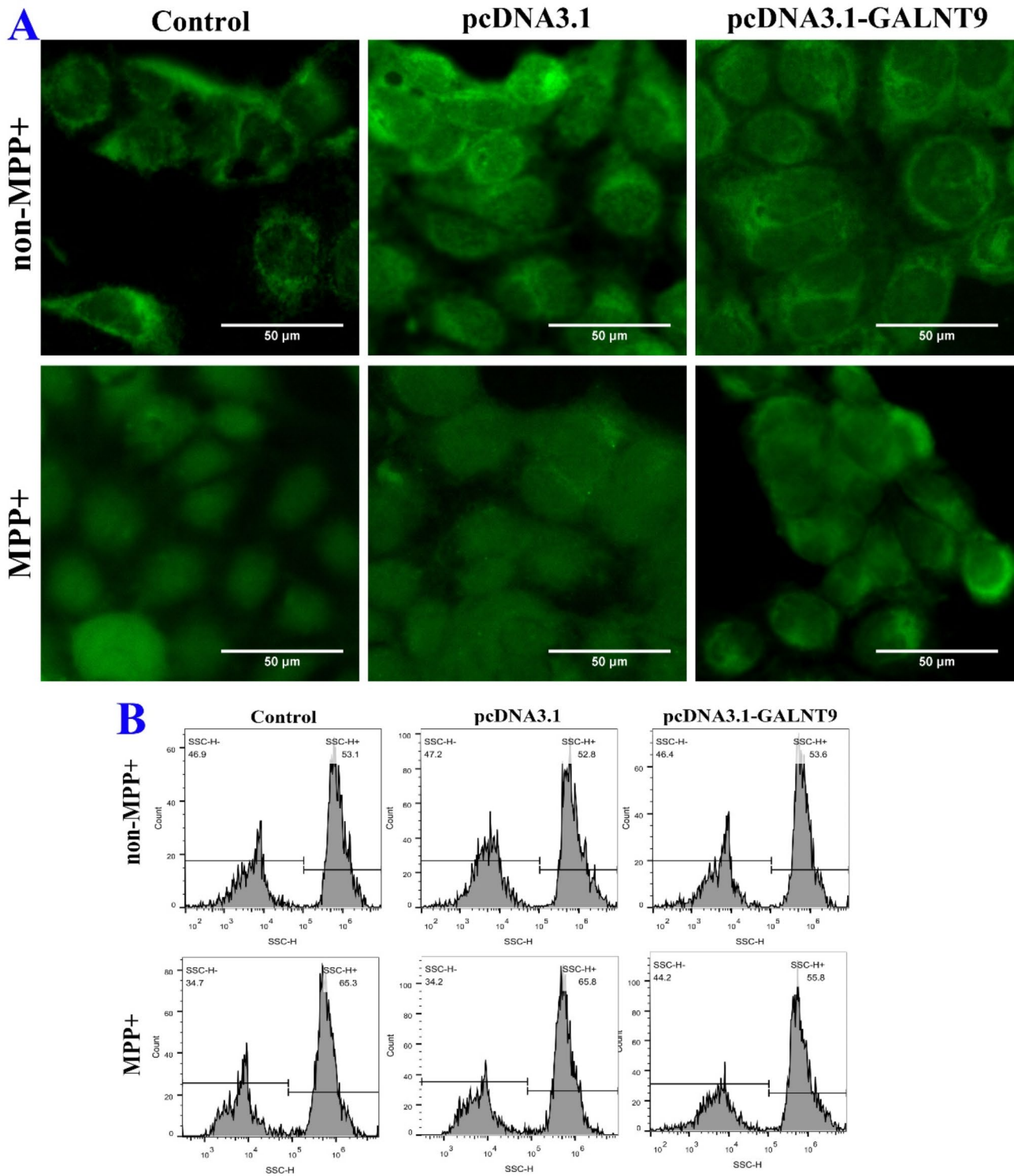
Fig. 6 Evaluation of GALNT9 on mitochondrial membrane permeability. (**A**) Representative images of mPTPs measured by fluorescence microscopy. A fluorogenic dye of calcein-AM/cobalt was used. The dimension of images was 429.33 mm × 429.33 mm. Examinations were performed in triplicate at least. The marked circular distribution of bright green fluorescent signals indicates mPTPs in a closed configuration. (**B**) Representative images of cytosolic Ca^{2+} measured by flow cytometry. Examinations were performed in quadruplicate. Fluo-4 AM was used as a probe. The rates of FITC-positive cells (which indicate leakage of Ca^{2+}) are shown

GALNT9 enrichment attenuated programmed cell death mediated by CytC-associated apoptotic cascade and reduced mitophagy

Mitochondria play a crucial role in the regulation of programmed cell death (PCD), a physiological process in which molecular programs intrinsic to cells are activated to elicit their destruction. Excessive activation of the mitochondrial-dependent PCD pathway is associated with dopaminergic neurodegeneration [29]. Because increased mitochondrial membrane permeability is associated with CytC release, we evaluated the CytC-mediated apoptotic pathway. The CytC-associated apoptotic cascade includes four proteins: CytC, apoptotic protease-activating factor-1 (Apaf1), activated caspase-9 (CASP9), and activated caspase-3 (CASP3).

CytC

In this study, cytoplasmic CytC levels were evaluated using western blotting (mitochondria were removed before evaluation). As shown in Fig. 6C, MPP$^+$ treatment significantly increased CytC levels in SH-SY5Y cells. However, GALNT9 reversed the high level of CytC induced by MPP$^+$. Our study revealed that GALNT9 overexpression inhibited CytC release from mitochondria. Thus, these data suggest that GALNT9 enrichment significantly inhibits nonspecific CytC release from mitochondria.

Apaf1

Abundance of Apaf1 was evaluated by western blotting. Apaf-1 is tightly bound to ATP in its inactive form, but CytC binding leads to the binding of ATP to ADP, followed by activation of the CytC-involved apoptotic pathway. As shown in Fig. 6C, densitometric analysis revealed that MPP$^+$ treatment enhanced cytoplasmic Apaf1 levels. However, GALNT9 enrichment dramatically reduced Apaf1 expression in MPP$^+$-treated and untreated SH-SY5Y cells. Therefore, these data suggest that GALNT9 enrichment ameliorates the increased Apaf1 expression induced by MPP$^+$ in neuronal cells.

CASP9

CASP9 is an initiator caspase and downstream member of Apaf1 in the CytC-mediated apoptotic cascade. Active Apaf1 is involved in assembly of the apoptosome, where procaspase-9 molecules are recruited and activated. Therefore, we evaluated the abundance of active CASP9 using western blotting. As shown in Fig. 6C, statistical analysis revealed an intense increase in active CAPS9 levels in MPP$^+$-treated cells compared to that in non-MPP$^+$-treated cells. However, GALNT9 enrichment greatly decreased active CASP9 levels under MPP$^+$ stress. Based on these data, GALNT9 enrichment was found to significantly decrease active CAPS9 levels.

CASP3

Activated CASP3, including 17 and 19 kDa molecules, was evaluated by western blotting. As shown in Fig. 6C, two bands were detected using a monoclonal anti-activated CASP3 antibody. Total densities were statistically summed to evaluate activated CASP3 levels. A significant increase in total activated CASP3 was observed in MPP$^+$-treated cells relative to untreated cells, signifying that MPP$^+$ treatment facilitated the cleavage of pro-CASP3. However, the high levels of activated CASP3 induced by MPP$^+$ were ameliorated by GALNT9 overexpression. These findings imply that GALNT9 enrichment can significantly downregulate activated CAPS3 levels.

Notably, these findings imply that GALNT9 enrichment leads to reduced cell apoptosis mediated by the CytC-mediated apoptotic pathway. This observation is consistent with our results of apoptosis determinations using Annexin V-FITC/PI assays.

Based on these findings, we speculated that GALNT9 enrichment allowed healthy cell growth via correct glycosylation of proteins, so that the number of cells with abnormal phenotypes, such as cellular shrinkage, membrane blebbing, and nuclear condensation, would be greatly decreased. Therefore, fewer cells need to be cleared via CytC-associated PCD. Hence, we observed a low apoptotic rate, as evaluated by Annexin V-FITC/PI assays, and identified attenuated activity of the CytC-associated apoptotic pathway when GALNT9 was overexpressed. Thus, GALNT9 enrichment confers a protective role in cell survival, and protein O-glycosylation plays a fundamental role in maintaining healthy cells.

MPTP triggers the release of CytC, a mitochondrial apoptogenic factor, followed by activation of CASP9 and CASP3 to enhance caspase-dependent PCD [30]. Our study of the CytC-associated pathway is in agreement with these reports. Our study consistently showed that treatment with MPP$^+$, an active form of MPTP in vivo, facilitated the release of CytC, leading to enhanced caspase-dependent PCD. In addition, the mechanism of CytC release involves mPTP opening [27]. In this study, we detected long-lasting mPTP opening under MPP$^+$ treatment, and more CytC was released into the cytosol. In addition, aggregated α-synuclein is reported to play a role in inducing CytC release to kill dopaminergic neurons by PCD [27, 31]. In this study, we clearly found that aggregated α-synuclein was present in cells treated with MPP$^+$, and that more CytC was detected in the cytosol. Based on the evidence obtained surrounding the CytC-associated pathway in this study, we believe that MPP$^+$ treatment enhances PCD mediated by the CytC-associated apoptotic pathway, as there were cells that required rapid clearance. However, GALNT9 enrichment played a role in maintaining healthy cells; thus, the decreased

number of unhealthy cells was associated with the low activity of the CytC-associated apoptotic pathway. This hypothesis was verified by the detection of mitophagy.

Mitophagy

Mitophagy is an autophagic process where damaged or aged mitochondria are selectively sequestered and eliminated [32, 33]. This process is essential for cellular homeostasis, metabolism, and development. Usually, appropriate mitophagy plays a pivotal role in neuronal homeostasis, whereas defects in mitophagy are associated with degenerative disorders, such as PD and Alzheimer's diseases [33–36]. Given the importance of mitophagy in cellular homeostasis and in degenerative disorders, we evaluated mitophagy using dual immunofluorescence staining. As shown in Fig. 7B, lysosomes are displayed in bright green, mitochondria are indicated as bright red, and mitochondria fused with lysosomes are displayed as bright yellow or orange by merged colors. Subsequently, we found that MPP^+ treatment led to bright yellow or orange spots with a largely rounded shape, whereas there were no clearly visible yellow or orange spots in non-MPP^+-treated cells. Under MPP^+ conditions, GALNT9 enrichment significantly reduced the numbers of merged color spots induced by MPP^+ treatment.
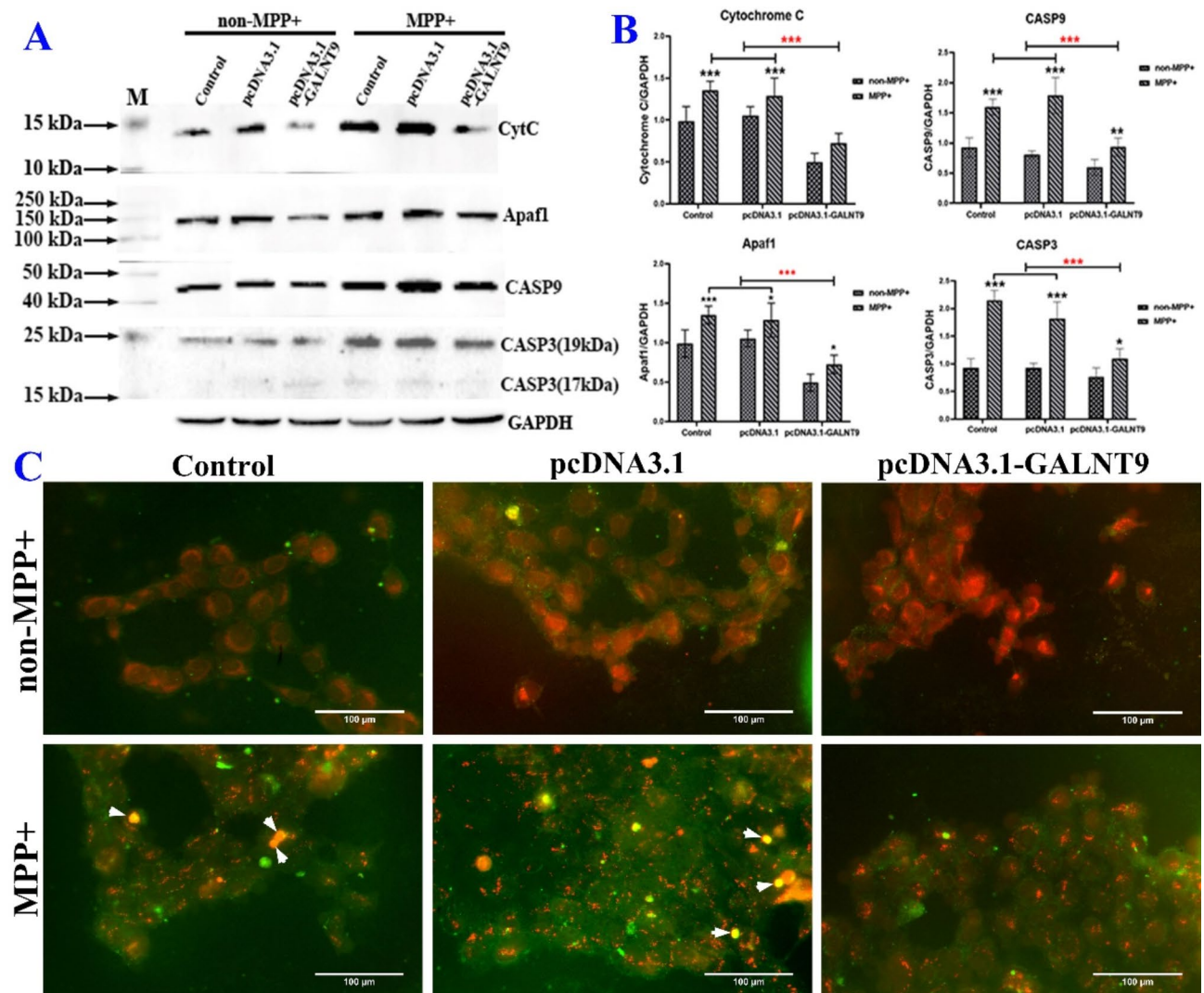

Fig. 7 Evaluation of mitophagy and PCD involved in CytC-associated apoptotic pathway. (**A**) Evaluation of molecules in CytC-associated apoptotic pathway by western blot assay. M, PageRuler prestained protein ladder (Yamei WJ103). Protein bands were normalized to GAPDH levels. Examinations was performed in triplicate at least. (**B**) Statistical analysis of expression of molecules including CytC, Apaf1, CASP9, and CASP3, respectively. Red asterisks represent comparison between GALNT9-regulated groups and controls, and black asterisks represent comparison between MPP^+-treated and -untreated groups. *, $P < 0.05$; **, $P < 0.01$; ***, $P < 0.001$. (**C**) Dual immunofluorescence staining of mitophagy. The dimension of micrographs was 1,731.43 mm × 1,151.47 mm. Green signals correspond to lysosomes. Red signals correspond to mitochondria. Mitochondrial fission is depicted as the juxtaposed images of green and red: dual immunolabelling of mitochondria/lysosomes is visible as orange or yellow indicated by white tips

These results indicated that GALNT9 enrichment ameliorated mitophagy induced by MPP$^+$. Specifically, these data concerning mitophagy are consistent with the evidence of CytC-associated apoptotic pathway involvement. MPP$^+$ exposure caused extensive cell damage, and such damaged cells could not be rapidly cleared via the CytC-mediated apoptotic pathway, even though the CytC-mediated apoptotic pathway was active under MPP$^+$ exposure. Finally, these damaged cells trigger excessive mitochondrial autophagy. However, GALNT9 overexpression maintained healthy cells via appropriate glycosylation. Thus, because there were fewer unhealthy cells, low activity of the CytC-associated apoptotic pathway was detected when GALNT9 was overexpressed. Similar to the effect of GALNT9 on the CytC-mediated apoptotic pathway, extremely weak mitophagy was observed in cells with GALNT9 enrichment. Therefore, we assumed that GALNT9 supplementation greatly ameliorated neuronal cell damage via O-GalNAc glycosylation under adverse conditions, which was supported by the observed low activity of the CytC-mediated apoptotic and mitochondrial autophagy pathways. Therefore, GALNT9 could potentially be developed as a therapeutic target in PD.

GALNT9, a mucin-type polypeptide *N*-acetylgalactosaminyltransferase 9, is a member of the GalNAc-transferase polypeptide GalNAc-transferase (GALNT) family. GALNTs catalyze the initial step of protein GalNAc-type O-glycosylation through linking an alpha *N*-acetylgalactosamine (α-GalNAc) from UDP-GalNAc to the hydroxyl group of a serine/threonine residue in a substrate polypeptide. GalNAc-type O-glycosylation occurs in any proteins that undergo passage through the secretory pathway [4, 37]. Mostly, O-glycosylated proteins are found on cell surface, in serum, and the extracellular matrix (ECM) [38]. Linked glycan moieties are essential for the structure, function, and properties of glycoproteins in living organisms. Altered glycosylation of cell surface O-glycoproteins is often associated with uncontrolled malignant cell proliferation, invasion, and metastasis. Aberrant O-GalNAc glycosylation of proteins is often linked to many diseases, such as carcinomas and central nervous system cancers [38].

Our study showed that soluble GALNT9 was downregulated exclusively in the brains of MPTP-treated mice. However, the total levels of GALNT9 increased in the midbrain and striatum. Considering the contradictory results obtained in this study, we speculate that the downregulation of soluble GALNT9 may result from GALNT9 deposition in insoluble forms. In addition, GALNT9 is specifically expressed in neurons under physiological conditions, whereas it is detected in glial cells under pathological conditions. Therefore, we assumed that increased total GALNT9 levels under pathological conditions possibly resulted from high levels of glial GALNT9. Therefore, glial GALNT9 has the potential to be developed as a pathogenic index in PD patients.

Based on the low levels of GALNT9 observed in tissues, we introduced a plasmid harboring overexpressed GALNT9 into neuronal cells to investigate whether GALNT9 supplementation played a role in ameliorating PD-like cytotoxicity. We found that GALNT9 supplementation ameliorated MPP$^+$-induced cytotoxicity through multiple pathways. Firstly, GALNT9 supplement decreased the protein aggregations formed by glycoproteins with terminal O-GalNAc and α-synuclein under MPP$^+$ exposure. Secondly, GALNT9 supplementation ameliorated the mitochondrial disorders induced by MPP$^+$ via alleviating aberrant levels of ΔΨm, ROS, providing sufficient ATP for maintaining dynamic assembly of actin cytoskeletons, and attenuating delayed opening of non-specific mitochondrial permeability pores. Third, GALNT9 enrichment maintained healthy cells, supported by few mitophagy events and low activity of the CytC-associated apoptotic pathway when GALNT9 was overexpressed in cells. Therefore, GALNT9 enrichment attenuates cytotoxicity under MPP$^+$ exposure and plays a therapeutic role in cells under pathological conditions. Thus, GALNT9 is a promising therapeutic target in PD.

GALNT9 plays an important role in ameliorating cytotoxicity induced by MPP$^+$. As a glycosyltransferase, the catalytic products of GALNT9 are glycoproteins with alpha O-GalNAc. Therefore, in this study, we detected glycoproteins using biotinylated DBA which specifically recognizes terminal alpha GalNAc moieties. However, after GALNT9 initiates the addition of the first GalNAc to a protein, the O-GalNAc of the glycoprotein undergoes subsequent extension and branching of the sugar chain in the Golgi apparatus, yielding several higher-order glycan structures [39]. Our study showed that MPP$^+$ treatment led to low levels of total DBA-recognized proteins. Based on a description of the structure of GalNAc-type O-glycosylation [39], it is supposed that MPP$^+$ treatment potentially attenuates initial O-GalNAcylation or promotes O-GalNAc to be further elongated/branched and capped by the sequential addition of monosaccharides. Abnormal O-GalNAcylation is associated with Parkinson's.

Conclusions
In conclusion, based on the finding that GALNT9 and its catalytic products are downregulated in animal and cellular models with PD-like variations, we investigated whether GALNT9 supplementation could ameliorate PD-like variations by introducing a recombinant plasmid, pcDNA3.1-*GALNT9*. We found that GALNT9 enrichment attenuated the cytotoxicity induced by MPP$^+$, which was supported by an increase in TH and DA levels

and a reduced rate of apoptosis when GALNT9 was over-expressed in cells.

To further explore the mechanism of action involved in GALNT9 ameliorating cytotoxicity induced by MPP$^+$ in neuronal cells, we investigated whether GALNT9 was involved in forming protein aggregates containing α-synuclein since α-synuclein aggregation is a hallmark of PD, and evaluated whether GALNT9 influences mitochondrial (dys)function since mitochondrial dysfunctions are commonly considered to represent fundamental pathogenic markers in PD. Consequently, it has been found that DBA-recognized proteins, potential catalytic products of GALNT9, are co-aggregated with α-synuclein under MPTP and MPP$^+$-induced conditions. However, GALNT9 enrichment dramatically reduces insoluble aggregates formed by DBA-recognized proteins and α-synuclein under MPP$^+$ treatment. In addition, our study showed that glial GALNT9 appears exclusively in animal brains with PD-like variations instead of neuronal GALNT9, suggesting that glial GALNT9 is associated with the pathogenesis of PD.

Our investigation of mitochondrial function, including metabolic energy generation and membrane permeability, demonstrated that GALNT9 enrichment ameliorated MPP$^+$-induced mitochondrial dysfunction by alleviating abnormal levels of ΔΨm and ROS, which are related to energy generation, and attenuating long-lasting mPTP opening and calcium efflux which are associated with mitochondrial membrane permeability. Finally, apoptosis analysis revealed that GALNT9 enrichment led to a low number of cells undergoing PCD, which was supported by the observed diminished activity of the CytC-associated apoptotic pathway and further inhibition of mitophagy.

This study reveals a crucial role of GALNT9 in the development of therapeutic strategies for PD-like variations.

Acknowledgements
Not applicable.

Declarations

Compliance with ethical standards
This study was carried out in accordance with the principles of the Basel Declaration and recommendations of Dalian Medical University for laboratory animals. The protocol was approved by the Animal Ethics Committee of Dalian Medical University.

Consent to participate
Not applicable.

Consent for publication
All authors consent to the publication of this manuscript.

Competing interests
The authors declare no competing interests.

Author details
[1]Biochemistry and Molecular Biology Department of College of Basic Medical Sciences, Dalian Medical University, Dalian 116044, China
[2]Department of Epidemiology, Dalian Medical University, Dalian 116044, China
[3]Department of Microbiology, Dalian Medical University, Dalian 116044, China
[4]Xiangyang Central Hospital, Affiliated Hospital of Hubei University of Arts and Science, Dalian, China

References
1. Wandall HH, Nielsen MAI, King-Smith S, de Haan N, Bagdonaite I. Global functions of O-glycosylation: promises and challenges in O-glycobiology. FEBS J. 2021;288(24):7183–212.
2. Brockhausen I, Stanley P. O-GalNAc glycans–essentials of glycobiology. Cold Spring Harbor (NY):Cold Spring Harbor Lab Press. 2017;3rd edition:Chap10.
3. Mereiter S, Balmaña M, Campos D, Gomes J, Reis CA. Glycosylation in the era of cancer-targeted therapy: where are we heading? Cancer Cell. 2019;36(1):6–16.
4. Bennett EP, Mandel U, Clausen H, Gerken TA, Fritz TA, Tabak LA. Control of mucin-type O-glycosylation: a classification of the polypeptide GalNAc-transferase gene family. Glycobiology. 2011;22(6):736–56.
5. Bloem BR, Okun MS, Klein C. Parkinson's disease. Lancet. 2021;397(10291):2284–303.
6. Weintraub D, Aarsland D, Chaudhuri KR, Dobkin RD, Leentjens AF, Rodriguez-Violante M, Schrag A. The neuropsychiatry of Parkinson's disease: advances and challenges. Lancet Neurol. 2022;21(1):89–102.
7. Tolosa E, Garrido A, Scholz SW, Poewe W. Challenges in the diagnosis of Parkinson's disease. Lancet Neurol. 2021;20(5):385–97.
8. Chen Y, Wu L, Liu J, Ma L, Zhang W. Adenine nucleotide translocase: current knowledge in post-translational modifications, regulations and pathological implications for human diseases. FASEB Journal: Official Publication Federation Am Soc Experimental Biology. 2023;37(6):e22953.
9. Toba S, Tenno M, Konishi M, Mikami T, Itoh N, Kurosaka A. Brain-specific expression of a novel human UDP-GalNAc:polypeptide N-acetylgalac-tosaminyltransferase (GalNAc-T9). Biochim et Biophys acta Bioenergetics. 2000;1493(1–2):264–8.
10. Peng Y, Wang C, Ma W, Chen Q, Xu G, Kong Y, Ma L, Ding W, Zhang W. Deficiency of polypeptide N-acetylgalactosamine transferase 9 contributes to a risk for Parkinson's disease via mitochondrial dysfunctions. Int J Biol Macromol. 2024;263.
11. Nakamura N, Toba S, Hirai M, Morishita S, Mikami T, Konishi M, Itoh N, Kurosaka A. Cloning and expression of a brain-specific putative UDP-GalNAc: polypeptide N-acetylgalactosaminyltransferase gene. Biol Pharm Bull. 2005;28(3):429–33.
12. Koeglsperger T, Rumpf S-L, Schließer P, Struebing FL, Brendel M, Levin J, Trenkwalder C, Höglinger GU, Herms J. Neuropathology of incidental Lewy body & prodromal Parkinson's disease. Mol Neurodegeneration. 2023;18(1).
13. Byrne J. Lewy body dementia. J R Soc Med. 1997;90(Suppl 32):14–5.

14. Koga S, Sekiya H, Kondru N, Ross OA, Dickson DW. Neuropathology and molecular diagnosis of synucleinopathies. Mol Neurodegeneration. 2021;16(1).
15. Hardy RE, Chung I, Yu Y, Loh SHY, Morone N, Soleilhavoup C, Travaglio M, Serreli R, Panman L, Cain K et al. The antipsychotic medications aripiprazole, brexpiprazole and cariprazine are off-target respiratory chain complex I inhibitors. Biol Direct. 2023;18(1).
16. Grimm A, Eckert A. Brain aging and neurodegeneration: from a mitochondrial point of view. J Neurochem. 2017;143(4):418–31.
17. Ammal Kaidery N, Thomas B. Current perspective of mitochondrial biology in Parkinson's disease. Neurochem Int. 2018;117:91–113.
18. Svitkina TM. Ultrastructure of the actin cytoskeleton. Curr Opin Cell Biol. 2018;54:1–8.
19. DeWane G, Salvi AM, DeMali KA. Fueling the cytoskeleton – links between cell metabolism and actin remodeling. J Cell Sci. 2021;134(3).
20. Gao J, Nakamura F. Actin-associated proteins and small molecules targeting the actin cytoskeleton. Int J Mol Sci. 2022;23(4).
21. De La Cruz EM, Gardel ML. Actin mechanics and fragmentation. J Biol Chem. 2015;290(28):17137–44.
22. Pollard TD, Borisy GG. Cellular motility driven by assembly and disassembly of actin filaments. Cell. 2003;112(4):453–65.
23. Daniel JL, Molish IR, Robkin L, Holmsen H. Nucleotide exchange between cytosolic ATP and F-actin-bound ADP may be a major energy-utilizing process in unstimulated platelets. Eur J Biochem. 1986;156(3):677–83.
24. Šileikytė J, Forte M. The mitochondrial permeability transition in mitochondrial disorders. Oxidative Med Cell Longev. 2019;2019:1–11.
25. Hurst S, Hoek J, Sheu S-S. Mitochondrial Ca2 + and regulation of the permeability transition pore. J Bioenerg Biomembr. 2016;49(1):27–47.
26. Bernardi P, Gerle C, Halestrap AP, Jonas EA, Karch J, Mnatsakanyan N, Pavlov E, Sheu S-S, Soukas AA. Identity, structure, and function of the mitochondrial permeability transition pore: controversies, consensus, recent advances, and future directions. Cell Death Differ. 2023;30(8):1869–85.
27. Perier C, Vila M. Mitochondrial biology and Parkinson's disease. Cold Spring Harbor Perspect Med. 2012;2(2):a009332.
28. Gleichmann M, attson MP. Neuronal calcium homeostasis and dysregulation. Antioxid Redox Signal. 2011;14(7):1261–73.
29. Vila M, Przedborski S. Targeting programmed cell death in neurodegenerative diseases. Nat Rev Neurosci. 2003;4(5):365–75.
30. Perier C, Tieu K, Guégan C, Caspersen C, Jackson-Lewis V, Carelli V, Martinuzzi A, Hirano M, Przedborski S, Vila M. Complex I deficiency primes bax-dependent neuronal apoptosis through mitochondrial oxidative damage. Proc Natl Acad Sci U S A. 2005;102(52):19126–31.
31. Parihar MS, Parihar A, Fujita M, Hashimoto M, Ghafourifar P. Alpha-synuclein overexpression and aggregation exacerbates impairment of mitochondrial functions by augmenting oxidative stress in human neuroblastoma cells. Int J Biochem Cell Biol. 2009;41(10):2015–24.
32. Tal R, Winter G, Ecker N, Klionsky DJ, Abeliovich H. Aup1p, a yeast mitochondrial protein phosphatase homolog, is required for efficient stationary phase mitophagy and cell survival. J Biol Chem. 2007;282(8):5617–24.
33. Evans CS, Holzbaur ELF. Autophagy and mitophagy in ALS. Neurobiol Dis. 2019;122:35–40.
34. Kitada T, Asakawa S, Hattori N, Matsumine H, Yamamura Y, Minoshima S, Yokochi M, Mizuno Y, Shimizu N. Mutations in the parkin gene cause autosomal recessive juvenile parkinsonism. Nature. 1998;392(6676):605–8.
35. Youle RJ, Narendra DP. Mechanisms of mitophagy. Nat Rev Mol Cell Biol. 2010;12(1):9–14.
36. Valente EM, Abou-Sleiman PM, Caputo V, Muqit MM, Harvey K, Gispert S, Ali Z, Del Turco D, Bentivoglio AR, Healy DG, et al. Hereditary early-onset Parkinson's disease caused by mutations in PINK1. Science. 2004;304(5674):1158–60.
37. Magalhães A, Duarte HO, Reis CA. The role of O-glycosylation in human disease. Mol Aspects Med. 2021;79.
38. Hussain MR, Hoessli DC, Fang M. N-acetylgalactosaminyltransferases in cancer. Oncotarget. 2016;7(33):54067–81.
39. Joshi HJ, Narimatsu Y, Schjoldager KT, Tytgat HLP, Aebi M, Clausen H, Halim A. SnapShot: O-glycosylation pathways across kingdoms. Cell. 2018;172(3):632–e2.

Publisher's note